International Journal of Applied Research 2018; 4(4): 115-123

ISSN Print: 2394-7500
ISSN Online: 2394-5869
Impact Factor: 5.2
IJAR 2018; 4(4): 115-123
www.allresearchjournal.com
Received: 01-02-2018
Accepted: 05-03-2018

Tahar Abbaz
Laboratory of Aquatic and Terrestrial Ecosystems, Org. and Bioorg. Chem. Group, University of Mohamed-Cherif Messaadia, Souk Ahras, Algeria, North Africa

Amel Bendjeddou
Laboratory of Aquatic and Terrestrial Ecosystems, Org. and Bioorg. Chem. Group, University of Mohamed-Cherif Messaadia, Souk Ahras, Algeria, North Africa

Didier Villemin
Laboratory of Molecular and Thio-Organic Chemistry, UMR CNRS 6507, INC3M, FR 3038, Labex EMC3, ensicaen & University of Caen, Caen France, Europe

Correspondence
Tahar Abbaz
Laboratory of Aquatic and Terrestrial Ecosystems, Org. and Bioorg. Chem. Group, University of Mohamed-Cherif Messaadia, Souk Ahras, Algeria, North Africa

The DFT study of tetrathiafulvalene connected to the amide and hydrazide functions (TTF-amide and hydrazide)

Tahar Abbaz, Amel Bendjeddou and Didier Villemin

Abstract
The geometrical behavior and structural stability of TTF-amide and hydrazide 1-4 were investigated by using density functional theory. Theoretical calculations were obtained by using B3LYP/6-31G(d,p) basis set. The HOMO and LUMO analysis are used to determine the charge transfer within the molecule. The stability of the molecule arising from hyper-conjugative interaction and charge delocalization has been analyzed using NBO analysis. Directly derived from density functional theory, the Fukui functions and the dual descriptor constitute powerful tools to get an insight into the chemical reactivity of a molecular system allowing to distinguish electrophilic and nucleophilic regions.

Keywords: tetrathiafulvalenes, density functional theory; computational chemistry, electronic structure quantum chemical calculations

1. Introduction
The TTF molecule, due to its unique π-donor properties, has been at the basis of many charge transfer salts with unique electronic and magnetic properties since its preparation [1] and the discovery of first organic conductors [2], more than 30 years ago. Its ability to form partially oxidized states gave rise to many molecular conductors [3], and in fact the large majority of organic metals and super-conductors known so far are based on TTF derivatives. One of the trends in the preparation of new TTF derivatives for electronic materials is the search for molecules with, simultaneously, more extended π-systems and an increasing number of sulfur atoms in the periphery, which can play a significant role in reducing the on-site Coulombic repulsion and increasing the strength and dimensionality of solid state interactions due to more S. S contacts. Since tetrathiafulvalene (TTF) was synthesized by Wudl *et al*. [4], it and its derivatives have been intensively investigated [5]. The covalent association of other functional groups (acceptor) with a strong electron donor-TTF unit can form D-A systems which are expected to generate intramolecular charge transfer between donor and acceptor unit [6].
In recent years, density functional theory (DFT) has been a shooting star in theoretical modeling. The development of better and better exchange-correlation functionals made it possible to calculate many molecular properties with comparable accuracies to traditional correlated ab initio methods, with more favorable computational costs [7].
The aim of the present work is to describe and characterize the molecular structure, the total energy, molecular frontier orbital energies (HOMO and LUMO), global chemical reactivity descriptors, molecular electrostatic potential maps (MEP), Fukui functions, the natural bonding orbital (NBO) analysis and nonlinear optics (NLO) properties of TTF-amide and hydrazide 1-4 illustrate in literature [8] by DFT method and B3LYP/6-31G (d, p) basis set.

2. Materials and Methods
Calculations of the TTF-amide and hydrazide 1-4 were carried out with Gaussian09 software [9] program using B3LYP/6-31G (d, p) basis set to predict the molecular structures. Calculations were carried out with Becke's three parameter hybrid model using the Lee-Yang-Parr correlation functional (B3LYP) method.

3. Results and Discussion

3.1. Molecular Geometry

The optimized parameters (bond lengths, bond angles and dihedral angles) of the title compounds were calculated at the DFT-B3LYP level with the 6-31G (d, p) basis set. The atom numbering of optimized structures is shown in Fig 1. The geometrical parameters were calculated and illustrated in Tables 1-4. All calculated geometrical parameters obtained at the DFT levels of theory are in correspond to true energy minima.

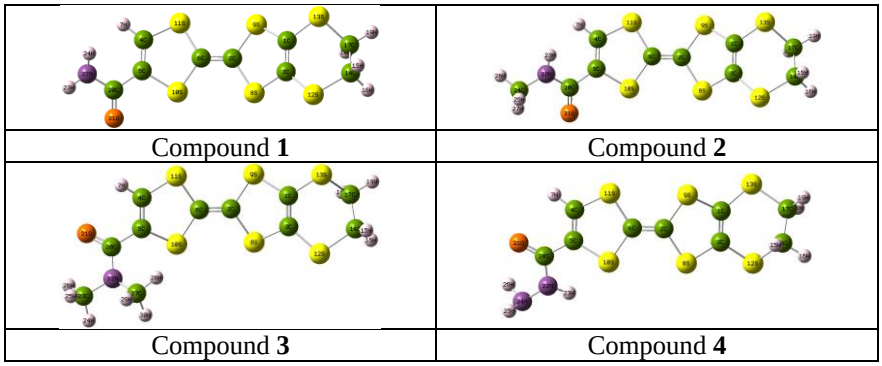

Fig 1: Optimized molecular structure of TTF-amide and hydrazide 1-4

Table 1: Optimized geometric parameters of compound **1**

Bond Length (Å)		Bond Angles (°)		Dihedral Angles (°)	
R(1,3)	1.349	A(3,1,9)	117.019	D(9,1,3,12)	177.598
R(1,9)	1.784	A(3,1,13)	123.846	D(6,2,9,1)	157.047
R(1,13)	1.762	A(9,1,13)	118.585	D(12,3,8,2)	167.238
R(2,6)	1.350	A(8,2,9)	112.669	D(8,3,12,14)	150.554
R(4,7)	1.083	A(1,3,8)	116.820	D(7,4,5,10)	173.900
R(4,11)	1.751	A(1,3,12)	127.745	D(7,4,11,6)	176.623
R(5,10)	1.774	A(8,3,12)	115.403	D(4,5,20,21)	159.118
R(5,20)	1.489	A(5,4,7)	124.505	D(10,5,20,22)	166.768
R(12,14)	1.862	A(2,6,11)	122.509	D(3,12,14,15)	116.669
R(13,17)	1.843	A(10,6,11)	113.831	D(1,13,17,18)	55.288
R(14,15)	1.091	A(3,12,14)	103.822	D(12,14,17,13)	54.419
R(14,17)	1.521	A(12,14,15)	106.135	D(12,14,17,19)	172.151
R(20,21)	1.223	A(15,14,16)	108.863	D(15,14,17,18)	171.982
R(20,22)	1.373	A(5,20,21)	120.913	D(16,14,17,13)	174.056
R(22,23)	1.010	A(20,22,23)	114.815	D(21,20,22,24)	154.638

Table 2: Optimized geometric parameters of compound **2**

Bond Length (Å)		Bond Angles (°)		Dihedral Angles (°)	
R(1,3)	1.349	A(3,1,9)	117.007	D(9,1,3,12)	177.627
R(1,9)	1.784	A(3,1,13)	123.953	D(6,2,9,1)	156.777
R(1,13)	1.763	A(9,1,13)	118.516	D(12,3,8,2)	167.068
R(2,6)	1.350	A(8,2,9)	112.635	D(8,3,12,14)	151.403
R(4,7)	1.083	A(1,3,8)	116.802	D(7,4,5,10)	173.664
R(4,11)	1.753	A(1,3,12)	127.878	D(7,4,11,6)	176.631
R(5,20)	1.493	A(8,3,12)	115.288	D(4,5,20,21)	155.825
R(12,14)	1.861	A(5,4,7)	124.659	D(10,5,20,22)	162.762
R(14,15)	1.091	A(10,5,20)	114.918	D(2,6,10,5)	166.345
R(14,17)	1.521	A(2,6,11)	122.549	D(3,12,14,15)	115.746
R(20,21)	1.227	A(10,6,11)	113.794	D(1,13,17,19)	171.786
R(20,22)	1.367	A(2,8,3)	93.542	D(12,14,17,13)	55.006
R(22,23)	1.008	A(4,11,6)	94.206	D(15,14,17,19)	52.098
R(22,24)	1.454	A(3,12,14)	103.839	D(21,20,22,23)	163.634
R(24,25)	1.097	A(15,14,16)	108.847	D(20,22,24,25)	93.728

Table 3: Optimized geometric parameters of compound **3**

Bond Length (Å)		Bond Angles (°)		Dihedral Angles (°)	
R(1,3)	1.349	A(3,1,9)	117.065	D(9,1,3,12)	177.687
R(1,9)	1.784	A(3,1,13)	123.954	D(8,2,6,11)	179.878
R(1,13)	1.763	A(9,1,13)	118.458	D(6,2,9,1)	156.714
R(2,6)	1.350	A(8,2,9)	112.643	D(12,3,8,2)	167.029
R(4,7)	1.083	A(1,3,8)	116.743	D(8,3,12,14)	151.516
R(4,11)	1.748	A(1,3,12)	127.928	D(7,4,5,10)	174.122
R(5,20)	1.503	A(8,3,12)	115.295	D(3,12,14,15)	115.440

R(12,14)	1.861	A(5,4,11)	119.374	D(1,13,17,19)	171.786
R(13,17)	1.842	A(4,5,10)	115.839	D(1,13,17,18)	55.529
R(14,15)	1.091	A(4,5,20)	120.436	D(12,14,17,19)	172.881
R(14,17)	1.521	A(10,6,11)	113.459	D(15,14,17,19)	52.326
R(20,21)	1.228	A(2,8,3)	93.538	D(16,14,17,13)	174.757
R(20,22)	1.376	A(3,12,14)	103.830	D(20,22,23,24)	150.817
R(22,23)	1.459	A(12,14,15)	106.268	D(27,22,23,25)	68.484
R(23,26)	1.088	A(15,14,16)	108.865	D(20,22,27,29)	104.831

Table 4: Optimized geometric parameters of compound **4**

Bond Length (Å)		**Bond Angles (°)**		**Dihedral Angles (°)**	
R(1,3)	1.349	A(3,1,9)	116.750	D(13,1,3,8)	177.656
R(1,9)	1.785	A(3,1,13)	127.809	D(13,1,9,2)	167.660
R(1,13)	1.763	A(6,2,8)	123.701	D(9,1,13,17)	150.592
R(2,6)	1.350	A(8,2,9)	112.784	D(8,2,6,11)	179.611
R(2,8)	1.780	A(1,3,8)	117.131	D(6,2,8,3)	158.099
R(3,12)	1.762	A(4,5,20)	121.482	D(20,5,10,6)	171.119
R(4,5)	1.343	A(10,6,11)	113.203	D(10,5,20,21)	165.106
R(4,7)	1.083	A(2,8,3)	93.609	D(2,6,11,4)	166.679
R(4,11)	1.747	A(3,12,14)	96.333	D(3,12,14,15)	55.429
R(5,20)	1.489	A(1,13,17)	103.798	D(1,13,17,18)	116.604
R(12,14)	1.843	A(12,14,15)	107.925	D(12,14,17,13)	54.400
R(14,15)	1.092	A(12,14,16)	105.993	D(12,14,17,19)	174.034
R(14,17)	1.521	A(15,14,17)	111.891	D(16,14,17,13)	172.076
R(20,21)	1.226	A(16,14,17)	109.143	D(21,20,22,23)	156.870
R(22,23)	1.011	A(20,22,23)	119.522	D(23,22,24,25)	125.231

3.2. Molecular Electrostatic Potential (MEP)

The molecular electrostatic potential is a well-established tool to explain the reactive behavior of a wide variety of chemical systems in both electrophilic and nucleophilic reactions, the study of biological recognition processes and hydrogen bonding interactions [10]. The electrostatic interaction between a molecule and a test charge of magnitude (that is a proton) placed at a point r is well represented by the molecular electrostatic potential V(r) using the equation:

$$V(r) = \sum_A \frac{Z_A}{|R_A - r|} - \int \frac{n(r')}{|r - r'|} dr'$$

Where Z_A is the charge on nucleus A located at R_A, n(r') is the electronic density function for the molecule and r' is the dummy integration variable [11,12]. At any given point r (x, y, z) in the vicinity of a molecule, the molecular electrostatic potential (MEP), the molecular electrostatic potential is related to electron density and a very useful descriptor for determining sites for electrophilic attack and nucleophilic reactions as well as hydrogen-bonding interactions [13]. To predict reactive sites for electrophilic and nucleophilic attack for the investigated molecule, the MEP at the B3LYP/6-31G (d, p) optimized geometry was calculated. The different values of the electrostatic potential at the surface are represented by different colors. Potential increases in the order red < orange < yellow < green < blue. The negative (red, orange and yellow) regions of the MEP are related to electrophilic reactivity. A visual representation of the chemically active sites and comparative reactivity of atoms of TTF-amide and hydrazide molecules is provides in Fig 2.

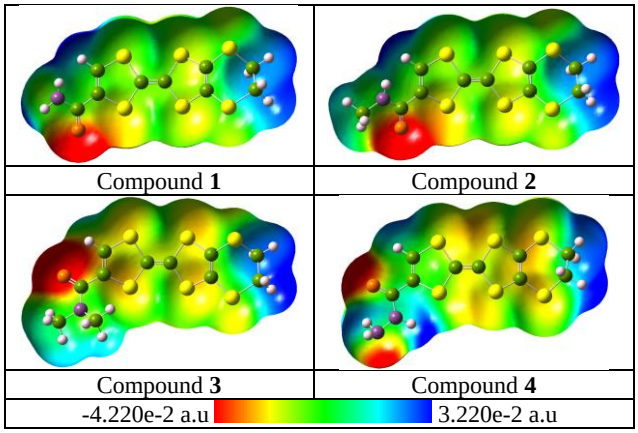

Fig 2: Molecular electrostatic potential surface of TTF- amide and hydrazide 1-4

As seen from the figure **2** that, in all molecules, the regions exhibiting the negative electrostatic potential are localized near the carbonyl group of amide function while the regions presenting the positive potential are localized vicinity of the

hydrogen atoms of cycled groups and hydrogen related to the nitrogen atom.

3.3. Frontier Molecular Orbitals (FMOs)

The energies of HOMO, LUMO, LUMO+1 and HOMO-1 and the energy gap of LUMO-HOMO are calculated using B3LYP/6-31G method and the pictorial illustration of the frontier molecular orbitals and their respective positive and negative regions are shown in Fig 3. The positive and negative phases are represented in yellow and blue color, respectively. Visual analysis of the molecular orbitals allows concepts of structural symmetry to be extended to frontier electron symmetry. It is actually possible to predict reactivity by examining the molecular orbitals [14,15]. The LUMO orbital feature a larger number of nodes than the HOMO orbital.

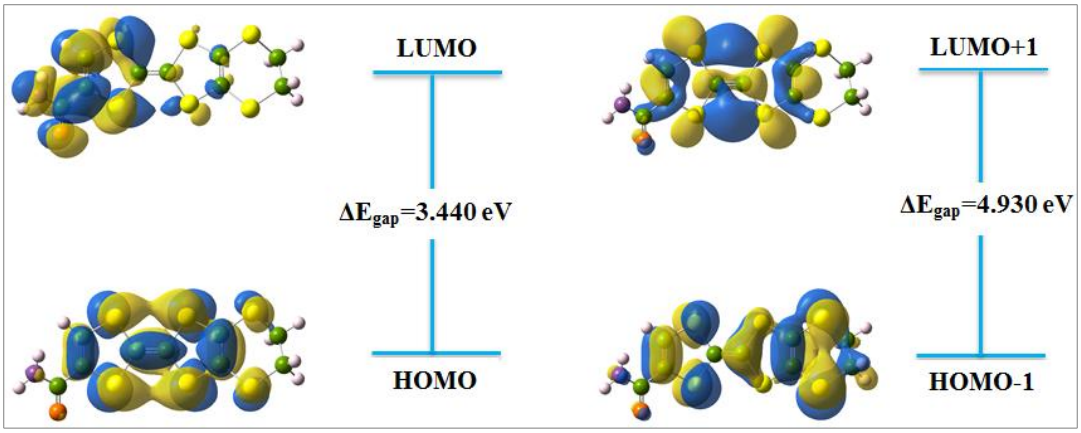

Fig 3: HOMO-LUMO Structure with the energy level diagram of compound 1

3.4. Global Reactivity Descriptors

Based on the density functional descriptors, global chemical reactivity descriptors of title molecule such as global hardness (η), chemical potential (μ), global softness (σ), electronegativity (χ), ionization potential (I), electron affinity (A) and global electrophilicity (ω) as well as local reactivity have been defined [16-19] as follows

$$\eta = \frac{1}{2}\left(\frac{\partial^2 E}{\partial N^2}\right)_{V(r)} = \frac{1}{2}\left(\frac{\partial \mu}{\partial N}\right)_{V(r)}$$

$$\mu = \left(\frac{\partial E}{\partial N}\right)_{V(r)}$$

$$\chi = -\mu = -\left(\frac{\partial E}{\partial N}\right)_{V(r)}$$

where E is the total energy, N is the number of electrons of the chemical species, μ is the chemical potential and V(r) is the external potential, which is identified as the negative of the electronegativity (χ) as defined by Iczkowski and Margrave [20]. According to Koop-man's theorem [21], the entries of the HOMO and the LUMO orbital's of the molecule are related to the ionization potential (I) and the electron affinity (A), respectively, by the following reactions:

$$I = -E_{HOMO}$$

$$A = -E_{LUMO}$$

Absolute electronegativity (χ) and absolute hardness (η) of the molecule are given by [22], respectively. Softness (*S*) is the reciprocal of hardness.

$$\chi = -\mu = \frac{1}{2}(I + A)$$

$$\eta = \frac{1}{2}(I - A)$$

$$S = \frac{1}{\eta}$$

Recently Parr *et al.* [23] have defined a new descriptor to quantity of global electrophilic power of the compound as electrophilicity index (ω) in terms of chemical potential and hardness as follows:

$$\omega = \left(\frac{\mu^2}{2\eta}\right)$$

All the calculated values of quantum chemical parameters of the molecules in B3LYP/6-31G basis set of DFT are presented in Table 5.

Table 5: Quantum chemical descriptors of TTF-amide and hydrazide **1-4**

Parameters	Compound 1	Compound 2	Compound 3	Compound 4
E_{HOMO} (eV)	-4.850	-4.813	-4.855	-4.992
E_{LUMO} (eV)	-1.410	-1.288	-1.130	-1.344
ΔE_{gap} (eV)	3.440	3.525	3.724	3.648
IE (eV)	4.850	4.813	4.855	4.992
A (eV)	1.410	1.288	1.130	1.344
μ (eV)	-3.130	-3.050	-2.993	-3.168
χ (eV)	3.130	3.050	2.993	3.168

η (eV)	1.720	1.763	1.862	1.824
S (eV)	0.291	0.284	0.269	0.274
ω (eV)	2.848	2.639	2.404	2.752

As presented in table 5, the compound which have the lowest energetic gap is the compound 1 (ΔE_{gap} = 3.440 eV). This lower gap allows it to be the softest molecule. The compound that have the highest energy gap is the compound 3 (ΔE_{gap} = 3.724 eV).The compound that has the highest HOMO energy is the compound 2 (E_{HOMO}= -4.813 eV). This higher energy allows it to be the best electron donor. The compound that has the lowest LUMO energy is the compound 1 (E_{LUMO} = -1.410 eV) which signifies that it can be the best electron acceptor. The two properties like I (potential ionization) and A (affinity) are so important, the determination of these two properties allow us to calculate the absolute electronegativity (χ) and the absolute hardness (η). These two parameters are related to the one-electron orbital energies of the HOMO and LUMO respectively. Compound 2 has lowest value of the potential ionization (*I* = 4.813 eV), so that will be the better electron donor. Compound 1 has the largest value of the affinity (A = 1.410 eV), so it is the better electron acceptor. The chemical reactivity varies with the structural of molecules. Chemical hardness (softness) value of compound **1** (η = 1.720 eV, **S** = 0.291 eV) is lesser (greater) among all the molecules. Thus, compound 1 is found to be more reactive than all the compounds. Compound 4 possesses higher electronegativity value (χ = 3.168 eV) than all compounds so; it is the best electron acceptor. The value of ω for compound 1 (ω = 2.848 eV) indicates that it is the stronger electrophiles than all compounds. Compound 1 has the smaller frontier orbital gap so, it is more polarizable and is associated with a high chemical reactivity, low kinetic stability and is also termed as soft molecule.

3.5. Local Reactivity Descriptors

The density functional theory (DFT) is a very useful framework for calculating local reactivity descriptors such as condensed Fukui function f (r) of the molecular system [24]. It is defined as the sensitivity of the electron density ρ(r) at various points in a species to a change in the number of electrons (N) in the molecular system at constant external potential υ(r) [24]. Thus, it was used to predict the variation in reactivity of different sites in a given molecule.

$$f(r)=\left(\frac{\partial\rho(r)}{\partial N}\right)_{\upsilon(r)} \quad (1)$$

Because of the discontinuity in the derivative at the N-value of Eq. (1), two definitions for Fukui function were introduced [25]:

$$f^{+}(r)=\left(\frac{\partial\rho(r)}{\partial N}\right)^{+}_{\upsilon(r)}$$ For a nucleophilic attack, and (2)

$$f^{-}(r)=\left(\frac{\partial\rho(r)}{\partial N}\right)^{-}_{\upsilon(r)}$$ For electrophilic attack (3)

Using the finite difference approximation, the above indices could be written as [15]:

$$f^{+}(r)=\rho^{N_0+1}(r)-\rho^{N_0}(r) \quad (4)$$

$$f^{-}(r)=\rho^{N_0}(r)-\rho^{N_0-1}(r) \quad (5)$$

where $\rho^{N_0}(r)$, $\rho^{N_0-1}(r)$ and $\rho^{N_0+1}(r)$ represent the electronic density function of neutral, cationic and anionic species, respectively, calculated at the same optimized geometry of the neutral species. The approximate integration of the Fukui function over atomic regions gives more informative function called condensed Fukui functions [26]. Consequently, the condensed Fukui functions are denoted as:

$$f_k^{+}=q_k^{N_0+1}-q_k^{N_0} \quad (6)$$

$$f_k^{-}=q_k^{N_0}-q_k^{N_0-1} \quad (7)$$

Where $q_k^{N_0}$, $q_k^{N_0-1}$and $q_k^{N_0+1}$ are the atomic electron populations at atom k for neutral, cationic and anionic species, respectively. Fukui functions for selected atomic sites in TTF-amide and hydrazide 1-4 are shown in Tables 6-7.

Table 6: Order of the reactive sites on compounds **1** and **2**

Compound 1					**Compound 2**				
Atom	6C	1C	3C	17C	Atom	6C	1C	3C	17C
f^{+}	0.060	0.010	0.005	-0.026	f^{+}	0.060	0.010	0.005	-0.025
Atom	3C	1C	6C	5C	Atom	3C	1C	6C	2C
f^{-}	0.025	0.015	0.010	0.008	f^{-}	0.026	0.014	0.012	0.007
Atom	6C	3C	1C	5C	Atom	3C	1C	6C	2C
f^{0}	0.035	0.015	0.012	-0.013	f^{0}	0.015	0.012	0.036	-0.014

Table 7: Order of the reactive sites on compounds **3** and **4**

Compound 3					**Compound 4**				
Atom	6C	5C	1C	3C	Atom	6C	3C	1C	2C
f^{+}	0.051	0.013	0.009	0.003	f^{+}	0.053	0.009	0.003	-0.017
Atom	3C	1C	6C	5C	Atom	1C	3C	5C	6C
f^{-}	0.025	0.015	0.014	0.009	f^{-}	0.025	0.013	0.011	0.010
Atom	6C	3C	1C	5C	Atom	6C	1C	3C	2C
f^{0}	0.032	0.014	0.012	0.011	f^{0}	0.032	0.014	0.011	-0.004

From the tables 6-7, the parameters of local reactivity descriptors show that 6C is the more reactive site in compounds 1, 2, 3 and 4 respectively for nucleophilic attacks. The more reactive sites for electrophilic attacks are 3C for compounds 1, 2 and 3 and 1C for compound 4 respectively. The more reactive sites in radical attacks are 6C for compounds 1, 3 and 4 and 3C for compound 2 respectively.

3.6. Natural Bond Orbital Analysis (NBO)

The NBO analysis is carried out by examining all possible interactions between 'filled'(donor) Lewis-type NBOs and 'empty'(acceptor) non-Lewis NBOs, and estimating their energetic important by 2nd order perturbation theory. Since these interactions lead to loss of occupancy from the localized NBOs of the idealized Lewis structure into the empty non-Lewis orbitals, they are referred to as delocalization corrections to the zeroth-order natural Lewis structure. For each donor NBO (i) and acceptor NBO (j) with delocalization i-j is estimated as

$$E^{(2)} = \Delta E_{ij} = q_i F(i,j)^2 / \varepsilon_j - \varepsilon_i$$

Where qi is the donor orbital occupancy ε_j and ε_i are diagonal elements orbital energies and F(i,j) is the off diagonal NBO Fock matrix element. The larger $E^{(2)}$ value, the more intensive is the interaction between electron donors and acceptors, i.e., the more donation tendency from electron donors to electron acceptors and the greater the extent of conjugation of the whole system. DFT (B3LYP/6-31G(d,p)) level computation is used to investigate the various second-order interactions between the filled orbitals of on Subsystem and vacant orbitals of another subsystem, which is a measure of the delocalization or hyper-conjugation [27]. NBOs are localized electron pair orbitals for bonding pairs and lone pairs. The hybridization of the atoms and the weight of each atom in each localized electron pair bond are calculated in the idealized Lewis structure. A normal Lewis structure would not leave any antibonding orbitals, so the presence of antibonding orbitals shows deviations from normal Lewis structures. Anti-bonding localized orbitals are called non-Lewis NBOs. This shows that the lone pair orbital participates in electron donation in the molecule. The calculated values of $E^{(2)}$ are shown in Tables 8-11.

Table 8: Second order perturbation theory analysis of Fock matrix on NBO of compound **1**

Donor(i)	ED/e	Acceptor(j)	ED/e	E(2)Kcal/mol	E(j)-E(i)a.u	F(i.j)a.u
LP(1)N22	1.77586	π*(C20-O21)	0.28177	41.56	0.32	0.105
LP(2)O21	1.85872	σ*(C20-N22)	0.06904	25.26	0.69	0.120
LP(2)S11	1.75083	π*(C4-C5)	0.25508	23.50	0.26	0.070
LP(2)S10	1.76851	π*(C4-C5)	0.25508	21.78	0.25	0.066
LP(2)O21	1.85872	σ*(C5-C20)	0.07346	20.58	0.66	0.106
LP(2)S8	1.79615	π*(C1-C3)	0.36691	19.64	0.24	0.063
LP(2)S9	1.79859	π*(C1-C3)	0.36691	19.30	0.24	0.063
LP(2)S12	1.85636	π*(C1-C3)	0.36691	17.24	0.24	0.061
LP(2)S10	1.76851	π*(C2-C6)	0.37726	16.86	0.25	0.061
LP(2)S11	1.75083	π*(C2-C6)	0.37726	15.72	0.26	0.059
π(C4-C5)	1.92354	π*(C20-O21)	0.28177	13.63	0.35	0.065
LP(2)S9	1.79859	π*(C2-C6)	0.37726	12.99	0.26	0.054
LP(2)S8	1.79615	π*(C2-C6)	0.37726	12.93	0.26	0.054
LP(2)S13	1.87498	π*(C1-C3)	0.36691	10.16	0.24	0.047
σ(C4-H7)	1.97476	σ*(C5-S10)	0.03015	5.90	0.76	0.060
σ(C1-S9)	1.97045	σ*(C3-S12)	0.02996	5.58	0.84	0.061
σ(C3-S8)	1.96871	σ*(C1-S13)	0.02937	5.30	0.84	0.060
σ(C2-S8)	1.96994	σ*(C6-S11)	0.04634	5.14	0.81	0.058
σ(C6-S11)	1.97286	σ*(C2-S8)	0.04528	5.14	0.83	0.058
σ(C6-S10)	1.97163	σ*(C2-S9)	0.04473	5.09	0.82	0.058

Table 9: Second order perturbation theory analysis of Fock matrix on NBO of compound **2**

Donor(i)	ED/e	Acceptor(j)	ED/e	E(2)Kcal/mol	E(j)-E(i)a.u	F(i.j)a.u
LP(1)N22	1.71762	π*(C20-O21)	0.30959	51.91	0.30	0.112
LP(2)O21	1.85594	σ*(C20-N22)	0.07521	25.12	0.71	0.122
LP(2)S11	1.75501	π*(C4-C5)	0.25326	22.93	0.26	0.069
LP(2)S10	1.76717	π*(C4-C5)	0.25326	21.78	0.25	0.066
LP(2)O21	1.85594	σ*(C5-C20)	0.07125	20.38	0.66	0.106
LP(2)S8	1.79706	π*(C1-C3)	0.36704	19.58	0.24	0.063
LP(2)S9	1.79936	π*(C1-C3)	0.36704	19.25	0.24	0.063
LP(2)S12	1.85619	π*(C1-C3)	0.36704	17.48	0.24	0.061
LP(2)S10	1.76717	π*(C2-C6)	0.37712	16.88	0.25	0.061
LP(2)S11	1.75501	π*(C2-C6)	0.37712	15.76	0.26	0.059
LP(2)S9	1.79936	π*(C2-C6)	0.37712	12.88	0.26	0.054
LP(2)S8	1.79706	π*(C2-C6)	0.37712	12.81	0.26	0.053
π(C4-C5)	1.92873	π*(C20-O21)	0.30959	12.74	0.35	0.063
LP(2)S13	1.87500	π*(C1-C3)	0.36704	10.27	0.24	0.047
LP(1)N22	1.71762	σ*(C24-H25)	0.01568	6.41	0.71	0.065
σ(C4-H7)	1.97469	σ*(C5-S10)	0.03033	5.87	0.76	0.060

σ(C1-S9)	1.97033	σ*(C3-S12)	0.03006	5.61	0.84	0.061
σ(C3-S8)	1.96856	σ*(C1-S13)	0.02948	5.32	0.84	0.060
σ(C6-S11)	1.97288	σ*(C2-S8)	0.04529	5.15	0.83	0.058
σ(C2-S8)	1.96998	σ*(C6-S11)	0.04616	5.13	0.81	0.058

Table 10: Second order perturbation theory analysis of Fock matrix on NBO of compound **3**

Donor(i)	ED/e	Acceptor(j)	ED/e	E(2)Kcal/mol	E(j)-E(i)a.u	F(i.j)a.u
LP(1)N22	1.68590	π*(C20-O21)	0.31122	49.08	0.29	0.106
LP(2)O21	1.85947	σ*(C20-N22)	0.07963	24.03	0.71	0.118
LP(2)S11	1.74921	π*(C4-C5)	0.23409	23.99	0.26	0.071
LP(2)O21	1.85947	σ*(C5-C20)	0.07394	21.11	0.65	0.106
LP(2)S9	1.79832	π*(C1-C3)	0.36679	19.41	0.24	0.063
LP(2)S8	1.79927	π*(C1-C3)	0.36679	19.32	0.24	0.063
LP(2)S10	1.78396	π*(C4-C5)	0.23409	18.62	0.26	0.062
LP(2)S12	1.85669	π*(C1-C3)	0.36679	17.47	0.24	0.061
LP(2)S11	1.74921	π*(C2-C6)	0.37976	16.73	0.26	0.061
LP(2)S10	1.78396	π*(C2-C6)	0.37976	16.49	0.26	0.061
LP(2)S9	1.79832	π*(C2-C6)	0.37976	12.83	0.25	0.053
LP(2)S8	1.79927	π*(C2-C6)	0.37976	12.64	0.26	0.053
π(C4-C5)	1.93058	π*(C20-O21)	0.31122	11.57	0.33	0.059
LP(2)S13	1.87426	π*(C1-C3)	0.36679	10.38	0.24	0.047
LP(1)N22	1.68590	σ*(C23-H25)	0.01705	6.48	0.70	0.065
σ(C4-H7)	1.97230	σ*(C5-S10)	0.03934	6.21	0.73	0.060
σ(C1-S9)	1.97020	σ*(C3-S12)	0.03014	5.62	0.84	0.061
LP(1)N22	1.68590	σ*(C27-H29)	0.01808	5.38	0.69	0.059
σ(C3-S8)	1.96864	σ*(C1-S13)	0.02941	5.31	0.84	0.060
σ(C2-S9)	1.97030	σ*(C6-S10)	0.04250	5.11	0.82	0.058

Table 11. Second order perturbation theory analysis of Fock matrix on NBO of compound **4**

Donor(i)	ED/e	Acceptor(j)	ED/e	E(2)Kcal/mol	E(j)-E(i)a.u	F(i.j)a.u
LP(2)S9	1.79520	π*(C1-C3)	0.36705	19.45	0.24	0.063
LP(2)S9	1.79520	π*(C1-C3)	0.36705	19.45	0.24	0.063
LP(2)S10	1.79296	π*(C4-C5)	0.24010	19.04	0.26	0.063
LP(2)S10	1.79296	π*(C4-C5)	0.24010	19.04	0.26	0.063
LP(2)S13	1.85591	π*(C1-C3)	0.36705	17.37	0.24	0.061
LP(2)S13	1.85591	π*(C1-C3)	0.36705	17.37	0.24	0.061
LP(2)S11	1.74638	π*(C2-C6)	0.37680	16.08	0.26	0.059
LP(2)S11	1.74638	π*(C2-C6)	0.37680	16.08	0.26	0.059
LP(2)S10	1.79296	π*(C2-C6)	0.37680	15.50	0.26	0.059
LP(2)S10	1.79296	π*(C2-C6)	0.37680	15.50	0.26	0.059
π(C4-C5)	1.91741	π*(C20-O21)	0.32382	15.13	0.33	0.067
LP(2)S8	1.79462	π*(C2-C6)	0.37680	13.65	0.25	0.055
LP(2)S9	1.79520	π*(C2-C6)	0.37680	13.40	0.26	0.055
LP(2)S12	1.87416	π*(C1-C3)	0.36705	10.29	0.24	0.047
LP(1)N24	1.96753	σ*(C20-N22)	0.08467	6.88	0.80	0.067
σ(C4-H7)	1.97220	σ*(C5-S10)	0.03839	6.39	0.73	0.061
σ(C3-S8)	1.97043	σ*(C1-S13)	0.02982	5.57	0.84	0.061
σ(C1-S9)	1.96891	σ*(C3-S12)	0.02912	5.28	0.84	0.059
σ(C2-S9)	1.97018	σ*(C6-S10)	0.04341	5.17	0.82	0.058
σ(C2-S8)	1.97020	σ*(C6-S11)	0.04531	5.15	0.81	0.058

The intra molecular interaction for the title compounds is formed by the orbital overl ap between: π(C4-C5) and π*(C20-O21) for compound 1, π(C4-C5) and π*(C20-O21) for compound 2, π(C4-C5) and π*(C20-O21) for compound 3 and π(C4-C5) and π*(C20-O21) for compound 4 respectively, which result into intermolecular charge transfer (ICT) causing stabilization of the system. The intra molecular hyper conjugative interactions of π(C4-C5) to π*(C20-O21) for compound 1, π(C4-C5) to π*(C20-O21) for compound 2, π(C4-C5) to π*(C20-O21) for compound 3 and π(C4-C5) to π*(C20-O21) for compound 4 lead to highest stabilization of 13.63, 12.74, 11.57 and 15.13 kJ mol^{-1} respectively. In case of LP(1)N22 orbital to the π*(C20-O21) for compound 1, LP(1)N22 orbital to π*(C20-O21) for compound 2, LP(1)N22 orbital to π*(C20-O21) for compound 3, LP(2)S9 orbital to π*(C1-C3) for compound 4 respectively, show the stabilization energy of 41.56, 51.91, 49.08 and 19.45 kJ mol^{-1} respectively.

3.7. Nonlinear Optical Properties (NLO)

Density functional theory has been used as an effective method to investigate the organic nonlinear optical materials. The NLO effects arise from the interactions of electromagnetic fields in various media to produce new fields altered in phase, frequency, amplitude or other propagation characteristics from the incident fields [28]. The polarizability and hyperpolarizability characterize the response of a system in an applied electric field [29]. They could determine not only the strength of molecular interactions (such as the long-range intermolecular

induction, and dispersion forces), the cross sections of different scattering and collision processes, but also the NLO of the system [30]. The theory of electric polarizability is a key element of the rational interpretation of a wide range of phenomena, from nonlinear optics and electron scattering [31] to phenomena induced by intermolecular interactions:

$$E = E^0 - \mu_\alpha F_\alpha - 1/2\alpha_{\alpha\beta}F_\alpha F_\beta - 1/6\beta_{\alpha\beta\gamma}F_\alpha F_\beta F_\gamma + \ldots$$

Where E^0 is the energy of unperturbed molecule, F_α the field at the origin, μ_α, $\alpha_{\alpha\beta}$ and $\beta_{\alpha\beta\gamma}$ are the components of dipole moment, polarizability and the first order hyperpolarizabilities, respectively. The total static dipole moment (μ), the mean diole polarizability (α), the anisotropy of the polarizability (Δα) and the total first order hyperpolarizability β_{total}, using x, y, z components they are defined as

$$\mu = \left[\mu_x^2 + \mu_y^2 + \mu_z^2\right]^{1/2}$$

$$\alpha = \left(\alpha_{xx} + \alpha_{yy} + \alpha_{zz}\right)/3$$

$$\Delta\alpha = 2^{-1/2}\left[\left(\alpha_{xx} - \alpha_{yy}\right)^2 + \left(\alpha_{yy} - \alpha_{zz}\right)^2 + \left(\alpha_{zz} - \alpha_{xx}\right)^2 + 6\alpha_{xx}^2\right]^{1/2}$$

$$\beta_{tot} = \left(\beta_x^2 + \beta_y^2 + \beta_z^2\right)^{1/2}$$

and

$$\beta_x = \beta_{xxx} + \beta_{xyz} + \beta_{xzz}$$

$$\beta_y = \beta_{yyy} + \beta_{xxy} + \beta_{yzz}$$

$$\beta_z = \beta_{zzz} + \beta_{xxz} + \beta_{yyz}$$

In the present work, the calculated dipole moment, polarizability and first order hyperpolarizability values are obtained and listed in Table 12.

Table 12: The dipole moments μ (D), polarizability α, the average polarizability α (esu), the anisotropy of the polarizability Δα (esu), and the first hyperpolarizability β (esu) of TTF-amide and hydrazide **1-4** calculated by B3LYP/6-31G(d,p) method

Parameters	Compound 1	Compound 2	Compound 3	Compound 4
β_{xxx}	12.4904	6.4151	-226.1633	-190.8483
B_{yyy}	9.1646	6.6966	4.5143	13.4296
B_{zzz}	8.2351	6.0931	2.5529	5.5102
B_{xyy}	2.2555	-7.2434	39.0194	18.4735
B_{xxy}	50.4592	36.5193	122.3222	-66.8337
B_{xxz}	89.1751	77.0948	18.9779	-18.1514
B_{xzz}	-31.0392	-23.0186	18.3557	16.8049
B_{yzz}	-2.4086	-23.0186	3.8313	-3.3751
B_{yyz}	4.8923	6.2921	7.8756	-3.4362
B_{xyz}	-0.6484	0.5343	-2.5560	7.4091
B_{tot}(esu)x10^{-33}	118.7767	93.1280	249.3825	176.7749
μ_x	1.2463	0.7249	-2.9529	-3.7600
μ_y	2.5273	2.4149	2.7430	-0.9515
μ_z	1.8179	1.9620	0.9834	-0.5194
μ_{tot}(D)	3.3534	3.1947	4.1486	3.9132
α_{xx}	-95.7424	-96.2496	-127.0441	-120.9984
α_{yy}	-147.7359	-152.8393	-151.0141	-148.4675
α_{zz}	-140.6474	-148.8768	-156.0570	-149.5197
α_{xy}	-18.2366	-18.1828	8.3429	0.1317
α_{xz}	-19.0790	-16.9505	10.9476	2.4024
α_{yz}	-0.0622	-0.6610	0.1483	1.6937
α(esu)x10^{-24}	66.8937	69.6346	35.9068	28.4699
$\Delta\alpha$(esu)x10^{-24}	9.9137	10.3198	5.3214	4.2192

Since the values of the polarizabilities (Δα) and the hyperpolarizabilities (β_{tot}) of the GAUSSIAN 09 output are obtained in atomic units (a.u.), the calculated values have been converted into electrostatic units (e.s.u.) (for α; 1 a.u = 0.1482 x 10^{-24} e.s.u., for β; 1 a.u = 8.6393 x 10^{-33} e.s.u.). The calculated values of dipole moment (μ) for the title compounds were found to be 3.3534, 3.1947, 4.1486 and 3.9132 D respectively, which are approximately four times than to the value for urea (μ = 1.3732 D). Urea is one of the prototypical molecules used in the study of the NLO properties of molecular systems. Therefore, it has been used frequently as a threshold value for comparative purposes. The calculated values of polarizability are 66.8937 x 10^{-24}, 69.6346 x 10^{-24}, 35.9068 x 10^{-24} and 28.4699 x 10^{-24} esu respectively; the values of anisotropy of the polarizability are 9.9137, 10.3198, 5.3214 and 4.2192 esu, respectively. The magnitude of the molecular hyperpolarizability (β) is one of important key factors in a NLO system. The DFT/6-31G(d,p) calculated first hyperpolarizability value (β) of TTF-amide and hydrazide molecules are equal to 118.7767 x 10^{-33}, 93.1280 x 10^{-33}, 249.3825 x 10^{-33} and 176.7749 x 10^{-33} esu. The first hyperpolarizability of title molecules is approximately 0.35, 0.27, 0.73 and 0.51 times than those of urea (β of urea is 343.272 x10^{-33} esu obtained by B3LYP/6-311G (d,p) method). The above results show that TTF-amide and hydrazide 1-4 might have not the NLO applications.

4. Conclusion

In the present study, the structural parameters for the optimized geometry of TTF-amide and hydrazide 1-4 have been obtained from DFT calculation. Nonlinear optical behavior of the examined compound was investigated by the determination of the electric dipole moment μ, the polarizability α and the hyperpolarizability β using the B3LYP method. So, it is demonstrated that the investigated compounds can be not used as a NLO material. The relative stabilities, HOMO-LUMO energy gaps and implications of

the electronic properties are examined. Additionally, the ionization potential (*I*), the electron affinity (A), the absolute electronegativity (χ), the absolute hardness (η) and softness (*S*) parameters were obtained from HOMO-LUMO energies of the investigated molecules.

Acknowledgments
This work was generously supported by the (General Directorate for Scientific Research and Technological Development, DGRS-DT) and Algerian Ministry of Scientific Research.

Reference

1. Wudl F, Smith GM, Hufnagel EJ. Bis-13-dithiolium chloride: an unusually stable organic radical cation. J Chem. Soc., Chem. Commun. 1970, 1453-1454.
2. Ferraris J, Cowan DO, Walatka Jr VV, Perlstein JH. Electron transfer in a new highly conducting donor-acceptor complex. J Am Chem. Soc. 1973; 95:948-949.
3. Yamada J. Sugimoto TTTF Chemistry fundamentals and applications of tetrathiafulvalene. Springer-Verlag. Berlin, 2004.
4. Wudl F, Smith G, Hufnagel E. Bis-1, 3-dithiolium chloride: an unusually stable organic radical cation. J Chem Soc D: Chem Commun, 1970, 1453-1454.
5. Jia C, Zhang J, Zhang L, Yao X. Structure-property relationships in conjugated donoreacceptor systems functionalized with tetrathiafulvalene. New J Chem. 2011; 35:1876-1882.
6. Takano Y, Herranz M, Martín N, Radhakrishnan S, Guldi D, Tsuchiya T. Donor-acceptor conjugates of lanthanum endohedral metallofullerene and pi-extended tetrathiafulvalene. J Am. Chem. Soc. 2010; 132:8048-8055.
7. Proft FD, Geerlings P. Conceptual and computational DFT in the study of aromaticity. Chem. Rev. 2001; 101:1451-1464.
8. Csuk R, Glänzer BI. Comprehensive heterocyclic chemistry II. Reference module in chemistry. Molecular Sciences and Chemical Engineering. 1996; 3:607-658.
9. Frisch MJ, Trucks GW, Schlegel HB. Gaussian09, Revision B.01, Gaussian Inc., Wallingford, CT. 2010.
10. Okulik N, Jubert AH. Theoretical analysis of the reactive sites of non-steroidal anti- inflammatory drugs. Internet Electron, J Mol. Des. 2005; 4:17-30.
11. Politzer P, Laurence PR, Jayasuriya K. Molecular electrostatic potentials: an effective tool for the elucidation of biochemical phenomena. Environ. Health Perspect. 1985; 61:191-202.
12. Politzer P, Lane PA. Computational study of some nitrofluoromethanes. Struct. Chem. 1990; 1:159-164.
13. Parlak C, Akdogan M, Yildirim G, Karagoz N, Budak E, Terzioglu C. Density functional theory study on the identification of 3-[(2-morpholinoethylimino)methyl]benzene-1,2-diol. Spectrochim. Acta, Part A. 2011; 79:263-271.
14. Seminario JM. Recent developments and applications of modern density functional theory. Elsevier. 1996; 4:800-806.
15. Yesilkaynak T, Binzet G, Mehmet Emen F, Florke U, Kulcu N, Arslan H. Theoretical and experimental studies on N-(6-methylpyridin-2-yl-carbamothioyl)biphenyl-4-carboxamide. Eur. J. Chem. 2010; 1:1-5.
16. Chattraj PK, Maiti B, Sarkar UJ. Philicity: a unified treatment of chemical reactivity and selectivity. J. Phys. Chem. 2003; 107:4973-4975.
17. Parr RG, Donnelly RA, Levy M, Palke WE. Electronegativity: the density functional viewpoint. J Am. Chem. Soc. 1978; 68:3801-3807.
18. Parr RG, Pearson RG. Absolute hardness: companion parameter to absolute electronegativity. J. Am. Chem. Soc. 1983; 105:7512-7516.
19. Parr RG, Chattraj PK. Principle of maximum hardness. J Am. Chem. Soc. 1991; 113:1854-1855.
20. Iczkowski RP, Margrave JV. Electronegativity. J Am. Chem. Soc. 1961; 83:3547-3551.
21. Larabi L, Harek Y, Benali O, Ghalam S. Hydrazide derivatives as corrosion inhibitors for mild steel in 1M HCl. Prog. Org. Coat. 2005; 54:256-262.
22. Lukovits I, Bako I, Shaban A, Kalman E. Polynomial model of the inhibition mechanism of thiourea derivatives. Electrochim. Acta. 1998; 43:131-136.
23. Parr RG, Szentpaly LV, Liu SJ. Electrophilicity index. Am. Chem. Soc. 1999; 121:1922-1924.
24. Parr RG, Yang W. Density functional approach to the frontier-electron theory of chemical reactivity. J. Am. Chem. Soc. 1984; 106:4049-4050.
25. Perdew JP, Parr RG, Levy M, Jr Balduz JL. Density-Functional theory for fractional particle number: derivative discontinuities of the energy. Phys. Rev. Lett. 1982; 49:1691.
26. Yang W, Mortier WJ. The use of global and local molecular parameters for the analysis of the gas-phase basicity of amines. J Am. Chem. Soc. 1986; 108:5708-5711.
27. Parthasarathi R, Padmanabhan J, Subramanian V, Sarkar U, Maiti B, Chattraj PK. Toxicity analysis of benzidine through chemical reactivity and selectivity profiles: a dft approach. Int. Electron J Mol. Des. 2003, 798-813.
28. Sun YX, Hao QL, Wei WX, Yu ZX, Lu LD, Wang X *et al.* Experimental and density functional studies on 4-(3,4-dihydroxybenzylideneamino)antipyrine, and 4-(2,3,4-trihydroxybenzylideneamino)antipyrine. J. Mol. Struct. (Thoechem). 2009; 904:7482.
29. Zhang QQ, Lei S, Wang X, Wang L, Yu P, Chen Y *et al.* Research on discrimination of 3D fluorescence spectra of phytoplanktons. Spectrosc. Spect. Anal. 2004; 24:1227-1229.
30. Christiansen O, Gauss J, Stanton JF. Frequency-dependent polarizabilities and first hyperpolarizabilities of CO and H_2O from coupled cluster calculations. Chem. Phys. Lett. 1999; 305:147-155.
31. Lane N. The theory of electron-molecule collisions. Rev. Mod. Phys. 1980; 52:29-120.